DAΦNE TECHNICAL NOTE

INFN - LNF, Accelerator Division

Frascati, Apr. 24, 1991

Note: **G-6**

A LOW LOSS CAVITY FOR THE DAΦNE MAIN RING

S. Bartalucci, L. Palumbo, B. Spataro

INTRODUCTION

One of the basic requirements of DAΦNE is an accelerating RF cavity with the lowest possible contents of higher order modes (HOMs). This is to minimize both single bunch and multibunch instabilities, which are a serious concern for the machine performances. Of course, cures of such instabilities must be envisaged and much effort is being presently put in on various techniques (damping, HOM tuning, RF active feedback etc.), which all aim at the same goal. However, we believe that a careful design of the cavity geometry is the primary step in this process.

We first observe that due to the low machine energy and the other relevant parameters, the power requirements are not very demanding. If we assume two resonators in each ring, a maximum voltage of 250 kV per cavity are needed. Since a reasonable upper limit on the power dissipation is 35 kW per cavity [1], the minimum required shunt impedance is $V^2/2P=0.9\ M\Omega$ per cavity, which is quite a low value. Thus, unlike most high energy electron storage rings, in our case the maximization of the shunt impedance is certainly not the main goal. A sacrifice in terms of shunt impedance is indeed acceptable, provided the HOM contents are drastically reduced. In this note we present a preliminary, theoretical study of a smooth-shaped, superconducting-like cell which might be a good candidate for the DAΦNE cavity.

TIME DOMAIN RESULTS

In 1983 T. Weiland proposed an accelerating cavity with large beam tubes as a single mode structure with only 27% reduction in shunt impedance [2]. We have adopted this design for our cell (which has to be normal conducting) and added two long tapers on both sides down to beam pipe radius of 3 cm. This design seems rather unconventional as compared to the usual geometry of superconducting structures, which include, besides the tapers, two straight, large- radius beam tubes where RF and HOM couplers are installed. The practical feasibility of this design has to be investigated much further but certainly there are not enormous difficulties.

Our criterion has been to minimize the cavity contribution to the impedance budget. The loss factor $k_T(\sigma_\tau)$ gives a good account for the real part of the impedance $Z_r(\omega)$. For a gaussian bunch it is given by:

$$k_T(\sigma_\tau) = \frac{1}{\pi}\int_0^\infty Z_r(\omega)\, e^{-\omega^2\sigma_\tau^2}\, d\omega \qquad [V/pC/cell]$$

In the time domain the relevant quantity is the 'bunch wakefield' for a charge distribution $\rho(\tau)$:

$$W_{/\!/}(\tau) = \frac{1}{\pi}\int_{-\infty}^{\tau} W_z(\tau-\tau')\, \rho(\tau')\, d\tau'$$

where Wz is the 'δ-function' longitudinal wakefield, or Green's function for a pointlike charge Q. The total loss factor due to the overall effect of monopole modes on a particle travelling on the symmetry axis of the cavity is naturally defined as

$$k_T = \frac{1}{Q^2}\int_{-\infty}^{+\infty} W_{/\!/}(\tau)\, \rho(\tau)\, d\tau \qquad [V/pC/cell]$$

and is numerically computed by codes like TBCI.

In the following we have chosen the structure physical length to be about 1.5 m. This value is by no means definitive, since the maximum available space in the present design of DAΦNE is about 2.6 m and some more space might be allowed for, if really needed.

The bare cell geometry is shown in Fig. 1, with superimposed the TBCI grid. The corresponding monopolar wakefield is shown in Fig. 2, up to a distance of 1 m from the head of the bunch. This and all the following calculations refer to a bunchlength of $\sigma_\tau = 0.1$ ns, or $\sigma_s = 3$ cm. The loss factor is found to be $k_T = 0.27$ V/pC. By inspection of Fig. 2 we observe that all parts of the bunch lose energy, and a big positive shoulder, corresponding to a regain of energy appears just after the bunch passage. This is due to the 'round' shape of the cell, where the accelerating gap and the cavity radius are of the same order of magnitude, so that the reflected wave has no time enough to strike back the bunch tail. Strong long-range wakefields exist at a distance of about 60 cm from the bunch centre, what is less than the wavelength of the accelerating mode $\lambda = 79$ cm. This suggests, in addition to the fundamental TM_{010}, the presence of a number of quite strong HOMs which have not decohered at the time of the next bunch passage. This situation certainly needs improvement from the point of view of both single-bunch and multibunch instabilities.

The idea is to 'open' the beam ducts and let the resonant region of the cavity be farther away from the beam line. The most natural step is to consider a geometry like the one depicted in Fig. 3, which makes use of the concept of 'large beam tube'. Because of the low cut-off frequency values (371 for TE and 780 MHz for TM modes), most HOMs have significant fields outside the cell region and their R/Q is thereby reduced. The resultant bunch wake is shown in Fig. 4 and the loss factor is k_T = 0.47 V/pC. This is a very high value, and reason is to be found in the abrupt transition ('step') from the beam pipe radius of 3 cm to the beam duct of 17 cm. In this case the excitation of very high frequency fields occurs through diffraction, and these modes extract much energy from the beam. On the contrary, the effect of the cavity modes is less important, as it can be clearly seen at a long distance. To get a confirmation of this concept, we have run TBCI for the beam ducts and steps only, without the accelerating cell (Figs 5-6). The loss factor is k_T = 0.38 V/pC, quite high, and also the wakefield profile shows a decohered tail on the long range. The single cell (Fig. 7) contribution is computed again by TBCI and found to be k_T = 0.07 V/pC. The corresponding wake is shown in Fig. 8 and displays the dominance of the fundamental mode, as expected. If the contributions of the structures as in Figs. 5 and 7 are added, a slight difference with the result of Fig. 4 is found. This can be attributed both to some numerical noise, which is always present in TBCI and to some interference effects, whose information is lost, when computing the two structures separately.

Since the main contribution to the loss factor comes from outside the accelerating cell, a gradual linear transition ('taper') has to be included in the geometry. This reduces the energy loss drastically, even for small taper length. In the case of infinitely long symmetric tapers k_T --> 0, while for an infinite single taper the limiting value is just half of the single step value.

In Fig. 9 the dependence of the loss factor on the taper length is shown for our cell geometry and two different lengths of the structure. When the taper length overcomes about 40 cm, the difference between the longer (114 cm half-length) and the shorter (74 cm) cavity becomes quite small and there's no clear need for a long cavity: cell contribution dominates. If the taper length is maximum for the 74 cm geometry, namely 55 cm, the loss factor is just 20% higher than the corresponding case for the 114 cm geometry (taper length 95 cm).

It is interesting to look at the effect of the taper only, without the accelerating cell. The geometry for the 55 cm - long taper is displayed in Fig. 10. The bunch wake (Fig. 11) exhibits a non-resonant, almost purely reactive behaviour along the bunch, where the tail regains the energy lost by the head. This explains the very small value of the loss factor (k_T = 0.04 V/pC), which is an average parameter. The long range term has disappeared almost completely.

Some energy spread, however, is introduced and the non-linear part must be considered carefully, while the linear part is automatically compensated by the RF system.

Finally, a comparison between a long-tapered cavity and a more conventional, short-tapered cavity was performed. The cavity profiles are shown in Fig. 12. The greater ability of the long taper to avoid the excitation of HOMs is shown clearly in Fig.13, where the electric field lines are 'photographed' when the bunch is about to leave the cavity. The stronger excitation of HOMs is represented by a greater number of field variations along the cavity gap and a larger line density in the short-tapered cavity. The wake potentials are compared in Fig.14. All the above remarks still apply, but it is interesting to note that even the energy spread is lower in the long-tapered cavity, as compared to the peak potential. The loss factors are found to be $k_T = 0.21$ and $k_T = 0.12$ V/pC, respectively, showing a definite preference for the long-tapered structure. This was further confirmed by computation of transverse wakefield. We report here only on the average transverse kick parameter k , which is the equivalent of the loss factor for the dipole modes and is given by

$$k = \frac{1}{Q^2}\int_{-\infty}^{+\infty} W(\tau)\,\rho(\tau)\,d\tau \qquad \left[V/(pC\ m)/cell\right]$$

The TBCI computed values are k = 4.76 V/(pC m) and k = 3.52 V/(pC m) for the short- and long-tapered cavity, respectively.

FREQUENCY DOMAIN RESULTS

That was all for the time domain calculations. The analysis was repeated in the frequency domain, by means of the well-known code URMEL. Owing to the huge CPU-time required by this code, especially when the highest available accuracy is used, we restricted ourselves to a comparison of the long and short-tapered cavities.

We have run URMEL for the short-tapered cavity up to about the cut-off frequency of the beam pipe, 3.82 GHz. This corresponds to 100 monopole modes, which are collected in Table I-a), with boundary conditions EM and in Table I-b), with boundary conditions MM. The loss factor for a bunchlength of 3 cm was computed according to the formula

$$k_T(\sigma_\tau) = \sum_n \frac{\omega_n}{2}\left(\frac{R_s}{Q}\right)_n e^{-\omega_n^2\sigma_\tau^2}$$

and a value $k_T = 0.16$ V/pC was found, showing a significant discrepancy with the TBCI result $k_T = 0.21$ V/pC. This may be ascribed to a worse accuracy (and high contamination) of the very high frequency modes computed by URMEL, but it is also likely to come from the presence of the above cut-off propagating modes, which are taken into account by TBCI.

Table I-a)

1SUMMARY OF ALL MODES FOUND (FULL CELL RESULTS)

(VOLTAGE INTEGRATED AT RO= 0.000 METER OFF AXIS)

MODE TYPE	FREQUENCY / MHZ	(R/Q)/OHM AT RO	ACCURACY	CONTAMINATION
TM0-EM- 1	380.957	38.987	9.4E-03	0.083615
TM0-EM- 2	717.908	0.284	1.8E-03	0.065703
TM0-EM- 3	794.570	3.571	1.1E-03	0.066333
TM0-EM- 4	941.790	1.933	7.9E-04	0.028776
TM0-EM- 5	1122.67	0.122	5.3E-04	0.042764
TM0-EM- 6	1186.17	0.323	6.1E-04	0.059932
TM0-EM- 7	1278.01	0.914	3.3E-04	0.024350
TM0-EM- 8	1414.46	5.206	2.6E-04	0.022188
TM0-EM- 9	1492.34	0.009	2.5E-04	0.027242
TM0-EM-10	1558.33	1.254	2.2E-04	0.035994
TM0-EM-11	1604.15	1.397	2.1E-04	0.037076
TM0-EM-12	1683.55	0.022	1.8E-04	0.036008
TM0-EM-13	1724.57	0.486	3.3E-04	0.071121
TM0-EM-14	1802.56	1.294	1.7E-04	0.025597
TM0-EM-15	1861.39	0.205	1.4E-04	0.030553
TM0-EM-16	1903.46	0.464	1.4E-04	0.033524
TM0-EM-17	2023.87	0.967	1.9E-04	0.180312
TM0-EM-18	2033.91	0.500	1.8E-04	0.183635
TM0-EM-19	2141.44	0.160	9.6E-05	0.017434
TM0-EM-20	2199.00	3.231	1.0E-04	0.115023
TM0-EM-21	2208.58	0.314	8.6E-05	0.103259
TM0-EM-22	2324.07	0.950	7.2E-05	0.030930
TM0-EM-23	2350.28	1.213	9.4E-05	0.042569
TM0-EM-24	2396.36	1.943	9.8E-05	0.025881
TM0-EM-25	2460.20	0.041	8.8E-05	0.027056
TM0-EM-26	2499.44	0.099	8.6E-05	0.034316
TM0-EM-27	2530.53	0.380	6.0E-05	0.029210
TM0-EM-28	2556.33	1.334	5.9E-05	0.127151
TM0-EM-29	2562.21	3.392	5.4E-05	0.119624
TM0-EM-30	2636.34	0.000	6.5E-05	0.027353
TM0-EM-31	2667.22	0.582	6.5E-05	0.028407
TM0-EM-32	2730.98	3.387	1.0E-04	0.032205
TM0-EM-33	2773.25	0.376	7.5E-05	0.047395
TM0-EM-34	2795.01	0.411	7.0E-05	0.045803
TM0-EM-35	2876.38	1.605	6.6E-05	0.026154
TM0-EM-36	2912.14	1.168	4.6E-05	0.036219
TM0-EM-37	2930.62	0.855	4.1E-04	0.328042
TM0-EM-38	2957.77	2.493	6.6E-05	0.036587
TM0-EM-39	3017.76	0.209	1.5E-04	0.039573
TM0-EM-40	3075.10	0.202	8.2E-04	0.516420
TM0-EM-41	3099.36	2.801	6.3E-03	4.020225
TM0-EM-42	3135.81	4.331	2.6E-03	1.145914
TM0-EM-43	3188.67	0.155	4.3E-02	10.000000
TM0-EM-44	3249.45	1.969	1.5E-02	6.807391
TM0-EM-45	3284.55	3.833	1.1E-02	5.058935
TM0-EM-46	3335.03	0.657	1.4E-02	4.522308
TM0-EM-47	3397.47	0.585	4.3E-02	10.000000
TM0-EM-48	3486.33	0.069	3.8E-02	7.617338
TM0-EM-49	3576.38	0.030	3.8E-02	7.742344
TM0-EM-50	3710.29	2.776	2.9E-02	3.952036

Table I-b)

0 0.00E+00 1.00E-01 2.00E-01 3.00E-01 4.00E-01 5.00E-01 6.00E-01 7.00E-01

1SUMMARY OF ALL MODES FOUND (FULL CELL RESULTS)

(VOLTAGE INTEGRATED AT RO= 0.000 METER OFF AXIS)

MODE TYPE	FREQUENCY / MHZ	(R/Q)/OHM AT RO	ACCURACY	CONTAMINATION
TM0-MM- 1	705.488	0.281	2.5E-03	0.117978
TM0-MM- 2	783.361	1.926	9.4E-04	0.052872
TM0-MM- 3	921.053	8.560	6.7E-04	0.024704
TM0-MM- 4	1063.24	3.078	6.9E-04	0.027979
TM0-MM- 5	1215.67	0.513	3.7E-04	0.016038
TM0-MM- 6	1375.08	0.445	3.6E-04	0.030514
TM0-MM- 7	1451.63	0.727	3.0E-04	0.029405
TM0-MM- 8	1570.31	0.339	2.4E-04	0.061786
TM0-MM- 9	1599.52	0.077	1.9E-04	0.054026
TM0-MM-10	1680.18	1.808	2.3E-04	0.026586
TM0-MM-11	1750.96	1.070	1.6E-04	0.030721
TM0-MM-12	1796.64	0.083	1.6E-04	0.031592
TM0-MM-13	1881.27	3.549	1.8E-04	0.024519
TM0-MM-14	1947.58	0.353	1.9E-04	0.027838
TM0-MM-15	2019.06	1.437	1.5E-04	0.022226
TM0-MM-16	2105.35	2.244	1.3E-04	0.035883
TM0-MM-17	2143.60	0.006	1.1E-04	0.061860
TM0-MM-18	2163.22	0.246	1.3E-04	0.072481
TM0-MM-19	2285.41	1.262	1.0E-04	0.040708
TM0-MM-20	2313.36	1.005	8.3E-05	0.035543
TM0-MM-21	2424.78	0.886	7.4E-05	0.110565
TM0-MM-22	2432.63	0.893	9.8E-05	0.153040
TM0-MM-23	2474.47	1.106	6.5E-05	0.039626
TM0-MM-24	2494.51	1.261	7.1E-05	0.044698
TM0-MM-25	2545.73	0.037	1.0E-04	0.025945
TM0-MM-26	2604.76	0.353	9.3E-05	0.025256
TM0-MM-27	2652.36	2.223	6.1E-05	0.034988
TM0-MM-28	2675.28	2.261	7.1E-05	0.042070
TM0-MM-29	2737.28	0.197	7.9E-05	0.017634
TM0-MM-30	2810.60	0.752	3.7E-05	0.031288
TM0-MM-31	2826.85	0.115	5.0E-05	0.044066
TM0-MM-32	2847.65	4.989	4.8E-05	0.033122
TM0-MM-33	2887.47	0.217	6.3E-05	0.023297
TM0-MM-34	2985.51	0.381	5.9E-05	0.027452
TM0-MM-35	3016.83	7.143	4.6E-05	0.031218
TM0-MM-36	3038.71	0.314	4.8E-05	0.034035
TM0-MM-37	3111.95	0.027	5.6E-05	0.017049
TM0-MM-38	3162.33	2.243	3.0E-03	2.498147
TM0-MM-39	3180.87	4.365	1.7E-03	1.850084
TM0-MM-40	3195.02	0.637	1.6E-03	1.813283
TM0-MM-41	3263.73	1.010	8.7E-04	0.285083
TM0-MM-42	3312.91	1.045	5.0E-03	3.327937
TM0-MM-43	3337.76	0.435	8.2E-03	5.612471
TM0-MM-44	3408.52	4.550	1.5E-02	9.659439
TM0-MM-45	3434.67	1.570	1.9E-02	10.000000
TM0-MM-46	3494.73	0.003	2.7E-02	8.455445
TM0-MM-47	3549.77	0.022	3.6E-02	10.000000
TM0-MM-48	3612.69	1.147	5.5E-02	10.000000
TM0-MM-49	3689.94	1.580	2.6E-02	6.413069
TM0-MM-50	3896.52	3.535	5.6E-02	5.131812

Table II-a)

1SUMMARY OF ALL MODES FOUND (FULL CELL RESULTS)

(VOLTAGE INTEGRATED AT RO= 0.000 METER OFF AXIS)

MODE TYPE	FREQUENCY / MHZ	(R/Q)/OHM AT RO	ACCURACY	CONTAMINATION
TM0-EM- 1	380.644	42.144	5.3E-03	0.045052
TM0-EM- 2	752.823	1.985	1.0E-03	0.019970
TM0-EM- 3	907.535	0.024	1.1E-03	0.037751
TM0-EM- 4	1099.24	0.185	1.4E-03	0.078034
TM0-EM- 5	1186.16	0.427	5.7E-04	0.040865
TM0-EM- 6	1278.22	1.336	4.3E-04	0.032237
TM0-EM- 7	1416.78	2.796	4.1E-04	0.035523
TM0-EM- 8	1494.83	0.031	8.7E-04	0.085764
TM0-EM- 9	1579.05	0.798	3.5E-04	0.033429
TM0-EM-10	1670.53	0.436	3.9E-04	0.039926
TM0-EM-11	1749.97	0.252	3.9E-04	0.045568
TM0-EM-12	1824.19	1.170	3.4E-04	0.055440
TM0-EM-13	1879.18	0.019	1.8E-04	0.031607
TM0-EM-14	1963.36	0.819	1.6E-04	0.020374
TM0-EM-15	2040.81	0.516	2.1E-04	0.028370
TM0-EM-16	2118.69	0.011	1.9E-04	0.038043
TM0-EM-17	2171.70	0.995	5.3E-04	0.133446
TM0-EM-18	2214.01	0.768	3.4E-04	0.091277
TM0-EM-19	2326.57	0.524	9.9E-03	2.447230
TM0-EM-20	2372.35	1.560	1.3E-02	3.305396

Table II-b)

1SUMMARY OF ALL MODES FOUND (FULL CELL RESULTS)

(VOLTAGE INTEGRATED AT RO= 0.000 METER OFF AXIS)

MODE TYPE	FREQUENCY / MHZ	(R/Q)/OHM AT RO	ACCURACY	CONTAMINATION
TM0-MM- 1	731.289	4.726	2.1E-03	0.053947
TM0-MM- 2	888.379	6.059	1.5E-03	0.048342
TM0-MM- 3	1044.56	1.204	2.1E-03	0.077001
TM0-MM- 4	1206.17	0.019	1.1E-03	0.045439
TM0-MM- 5	1380.35	0.575	7.5E-04	0.065654
TM0-MM- 6	1453.76	0.061	1.1E-03	0.118095
TM0-MM- 7	1573.89	0.770	8.3E-04	0.057123
TM0-MM- 8	1695.88	0.242	1.7E-03	0.243730
TM0-MM- 9	1751.52	1.299	2.8E-03	0.461396
TM0-MM-10	1840.17	0.000	2.3E-03	0.313222
TM0-MM-11	1906.52	2.751	3.9E-03	0.570091
TM0-MM-12	1996.92	0.124	3.1E-03	0.391552
TM0-MM-13	2074.28	2.079	2.3E-03	0.424801
TM0-MM-14	2130.02	0.049	1.2E-03	0.344261
TM0-MM-15	2166.54	0.084	2.9E-03	0.886162
TM0-MM-16	2258.87	0.776	4.1E-03	0.819193
TM0-MM-17	2314.64	0.375	1.4E-03	0.296866
TM0-MM-18	2434.65	1.712	1.1E-02	10.000000
TM0-MM-19	2445.08	0.023	1.2E-02	10.000000
TM0-MM-20	2555.71	1.366	3.2E-02	3.625765

As long as one believes in the computations of these codes, this comparison looks much more favourable for the long-tapered cavity. In this case, we ran URMEL only for 40 monopole modes, which are collected in Table II a), b). For such a number of modes, indeed, we have got k_T = 0.11 V/pC, which is clearly very close to the time-domain value k_T = 0.12 V/pC, thus we have decided to save on CPU-time. This result might be inaccurate, but certainly the absence of abrupt discontinuities in the beam tube prevents the excitation of the above cut-off HOMs more effectively.

The numerical results for the 2 geometries are summarized in Table III. Both resonate at the same frequency and have the same Q-factor values, while the characteristic impedance is a bit higher for the long-tapered structure. Accordingly, the loss factor of the fundamental mode k_0 is higher, but the contents of HOMs are definitely lower by more than a factor two, as given by the parasitic mode (pm) loss factor $k_{pm} = k_T - k_0$. In fact, we have k_{pm} = 0.07 V/pC for the long-tapered cavity and k_{pm} = 0.16 V/pC for the short-tapered one.

Table III

Comparison of the short- and long-tapered cavities

		Short-tapered	Long-tapered
f	(MHz)	381	381
R/Q	[Ω]	39	42
Q	48000	48000	
K_o	(V/pC)	0.044	0.048
k_T	(V/pC)	0.21	0.12
k_{pm}	(V/pC)	0.16	0.07

CONCLUSIONS

The long-tapered cavity constitutes a valuable starting point for the optimization study of the DAΦNE accelerating cavity. Even if the final design were very different from what we have presented in this note, we believe that the basic idea of the long taper has to be kept in mind, since it has all the advantages of the 'large beam tube' concept, whereas in DAΦNE we can neglect its main drawback, namely, the poor shunt impedance.

Furthermore, the contributions to the Broadband Impedance and to the Transverse Impedance are definitely lower, and this is a very important requirement for the machine.

The main problems to be faced are the RF power coupler, whose location has to be optimized, and the HOM damping technique. Several possibilities are presently under study, like the use of absorbing materials (ferrites, dielectrics with resistive coating, etc.). which provide global damping of all HOMs. An optimum position for these absorbers may be found, without affecting the fundamental mode significantly. In fact, if we compare the electric field profile of the fundamental mode (Fig.15) with the one of first monopole mode (Fig.16), we see that the latter has quite a lot of field lines in the taper region, where absorbers might be inserted. This approach is indeed presently pursued at Cornell [3], where ferrite materials were successfully tested on a prototype cavity for the B-Factory Project.
Another interesting possibility, which may be combined with the global damping technique, is the active HOM feedback. Its principle has already been successfully applied to strongly reducing the shunt impedance of the fundamental mode in a s.c. cavity, which is installed on the SPS for electron acceleration, and must be made 'invisible' to the beam during proton operation [4]. This approach look very promising, provided it can be applied to a limited number of HOMs. This seems to be our case, since in our design there are at least two dipole modes which do extend significantly outside the cell region and, in addition, there are the so-called 'trapped' monopole modes, which might be difficult to get rid of. A vigorous R&D program, mainly on electronics and controls, has to be carried on, anyway.

A further possibility is to combine the global damping technique with the HOM tuning. Preliminary tests on a pill-box have given very encouraging results [5], although much work is still to be done on this novel idea. Again, we can envisage to shift some low frequency dangerous modes, provided they are not damped too much by the absorbers, so that the HOM tuning is still effective.

As a general remark, we think that all possibilities must be investigated carefully, not only with laboratory tests but also with more sophisticated computer simulations, which are nowadays quite able to work with a very realistic design of a resonating structure.

REFERENCES

[1] R. Boni and A. Gallo, "The radiofrequency system for DAΦNE", DAΦNE Techn. Note, RF -1 (1990).
[2] T. Weiland, "Single Mode Cavities", DESY Report 83/073 (1983).
[3] H. Padamsee et al., "Superconducting RF Accelerating and Crab Cavities for the Cornell B-Factory, CESR-B", Cornell Un. Report, CLNS 90-1039 (1990).
[4] D. Boussard, H.P. Kindermann and V.Rossi, "RF Feedback applied to a Multicell Super-conducting Cavity", Proc. of European Part. Acc. Conference, Rome 7-11 June 1988, p. 985.
[5] S. Bartalucci et al.,"A Perturbation Method for HOM Tuning in a RF Cavity", DAΦNE Int. Note (in preparation) and subm. to Particle Accelerators.

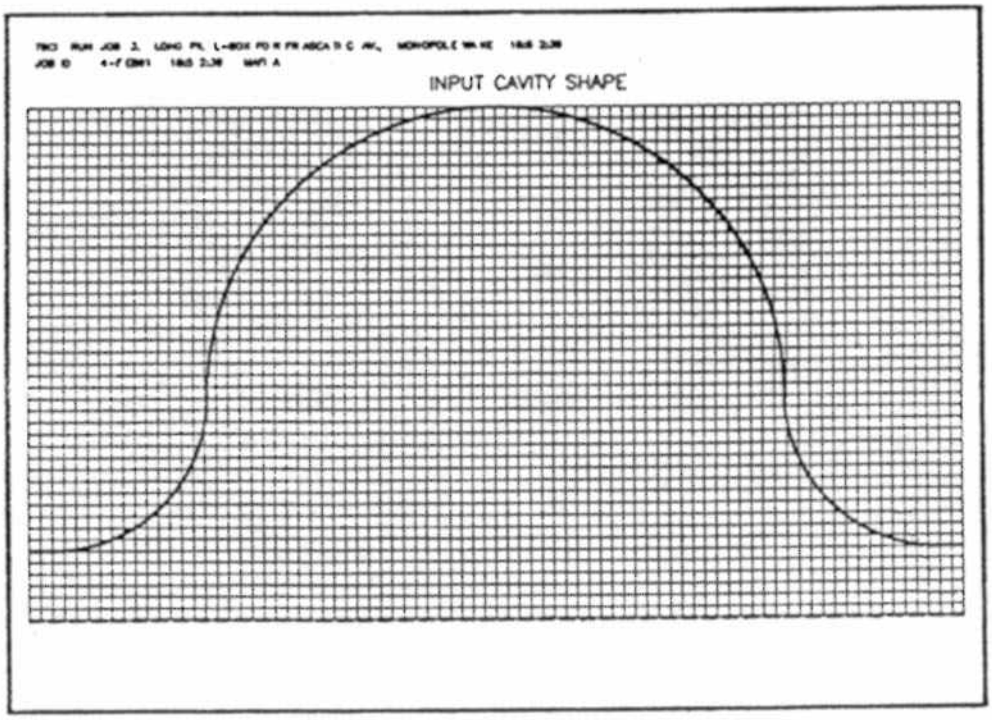

FIG. 1

$k_T = 0.266\ V/pC$

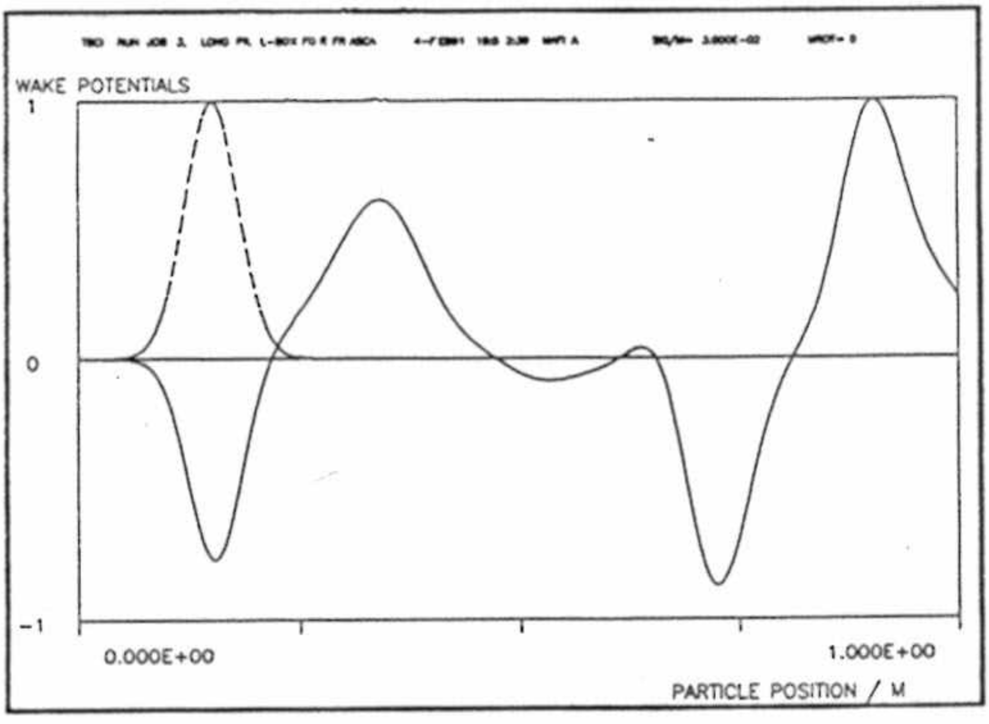

FIG. 2

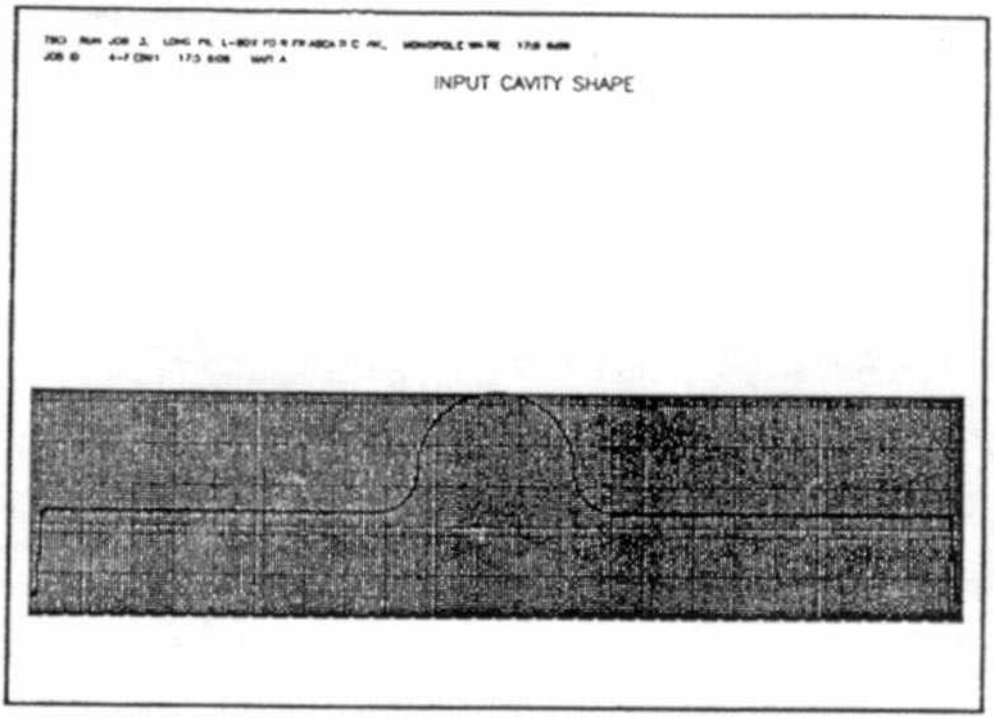

FIG. 3

$K_T = 0.467\ V/pC$

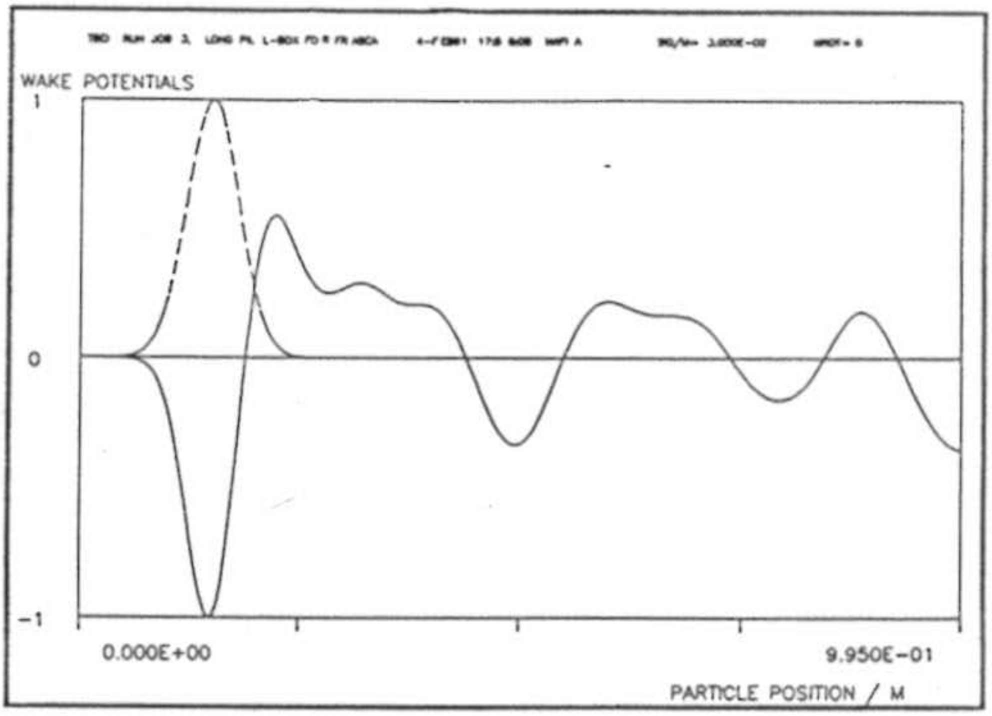

FIG. 4

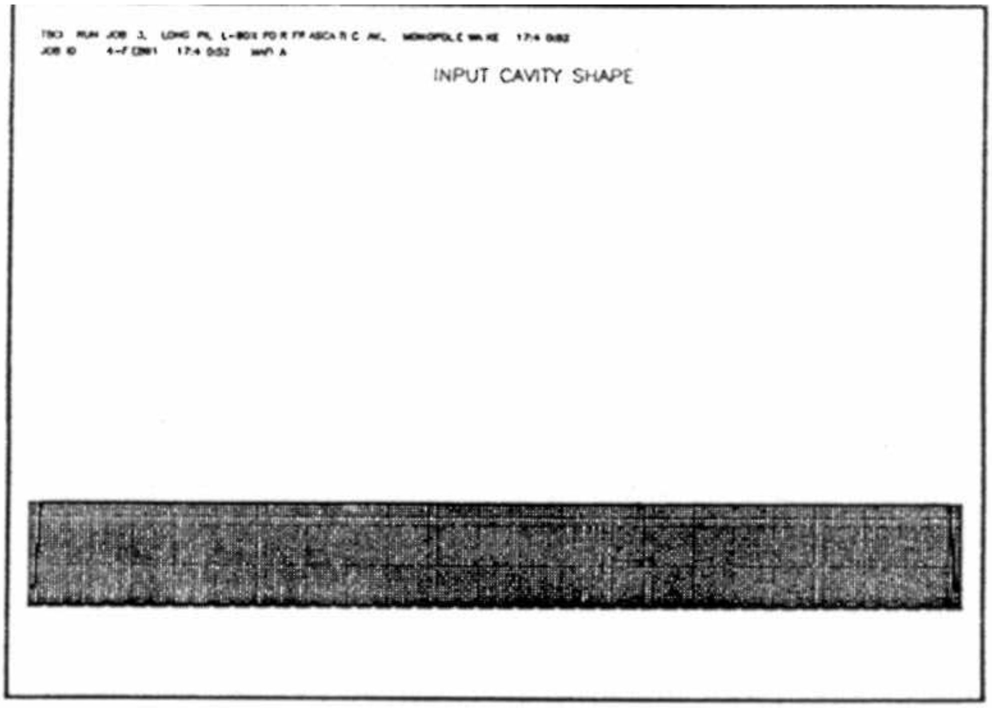

FIG. 5

$\kappa_T = 0.375$ V/p

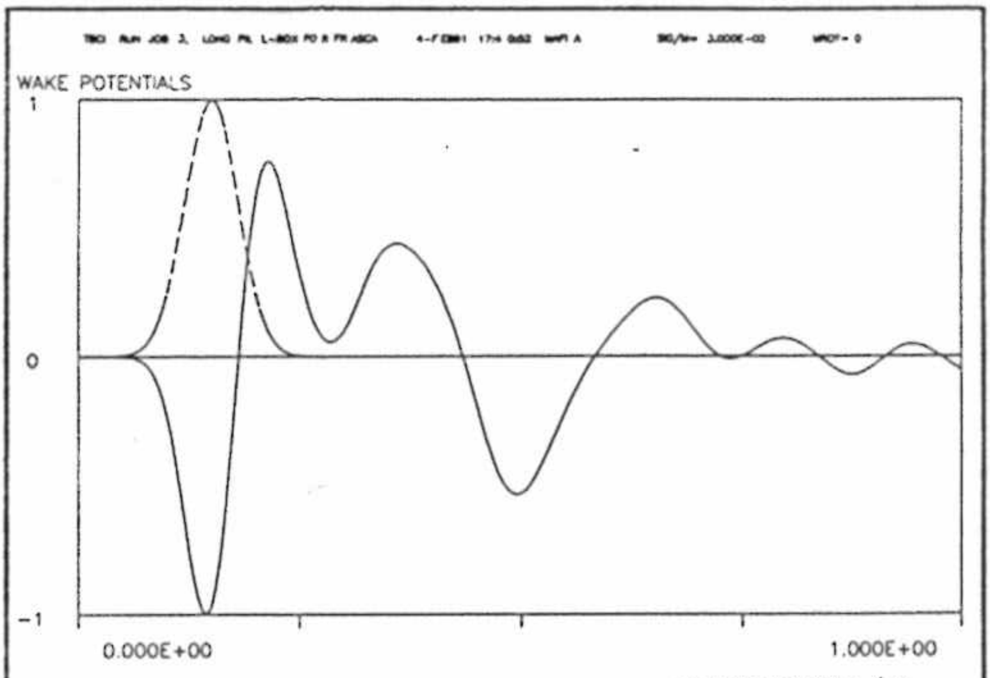

FIG. 6

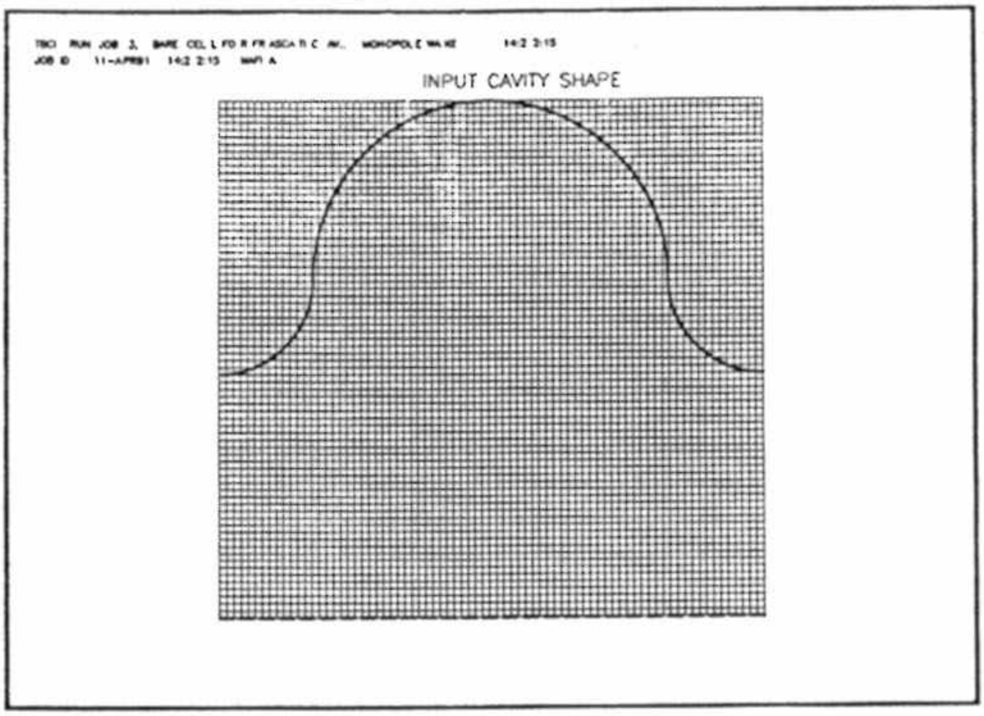
INPUT CAVITY SHAPE

FIG. 7

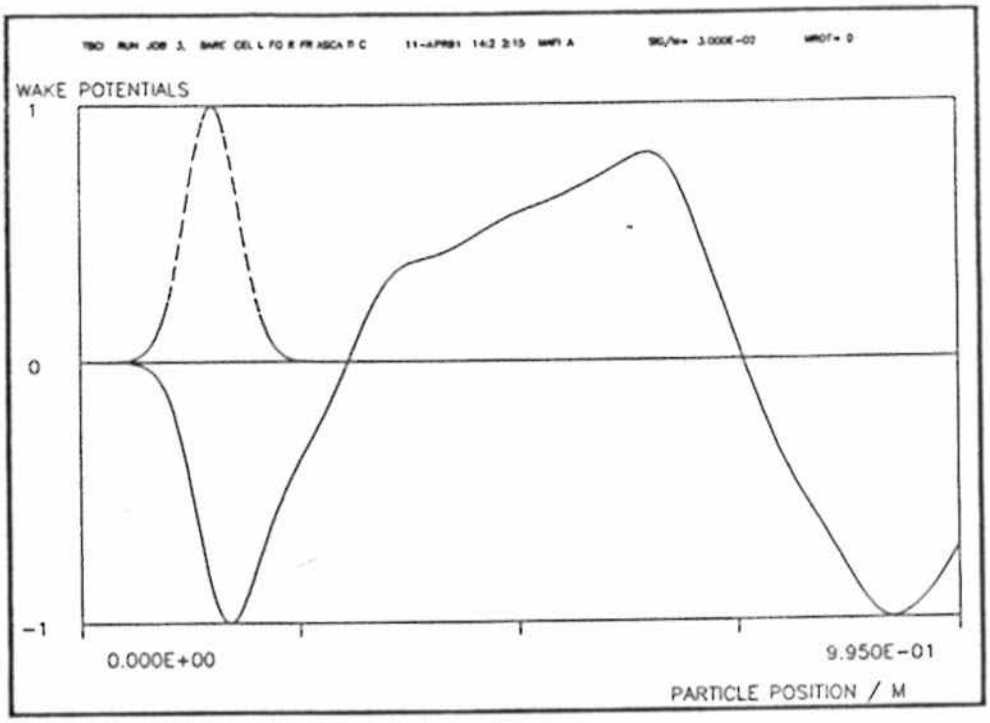
WAKE POTENTIALS
1
0
−1
0.000E+00
9.950E−01
PARTICLE POSITION / M

FIG. 8

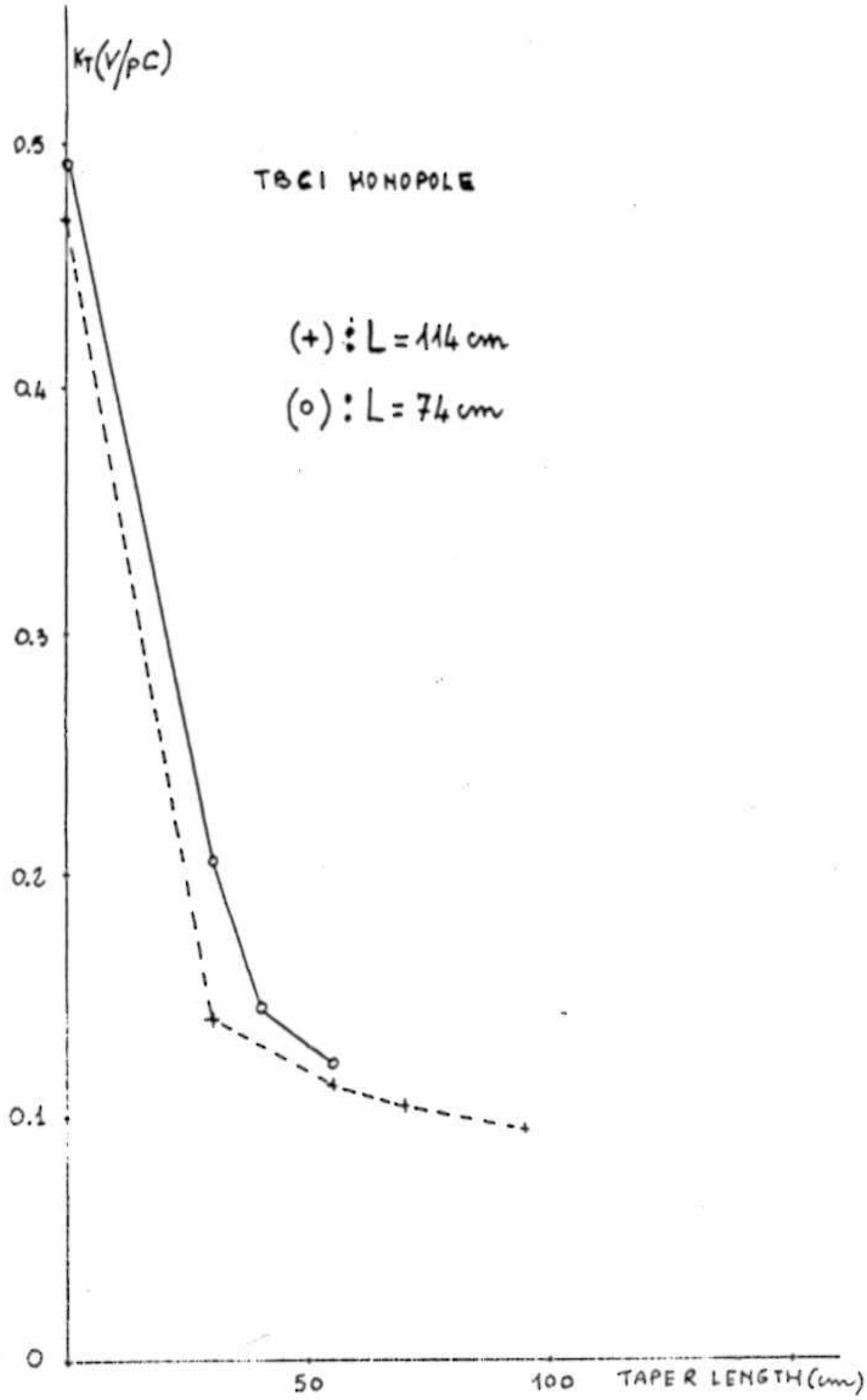
$K_T(V/pC)$
0.5
0.4
0.3
0.2
0.1
0
50
100
TAPER LENGTH (cm)
TBCI MONOPOLE
(+) : L = 114 cm
(o) : L = 74 cm

FIG. 9

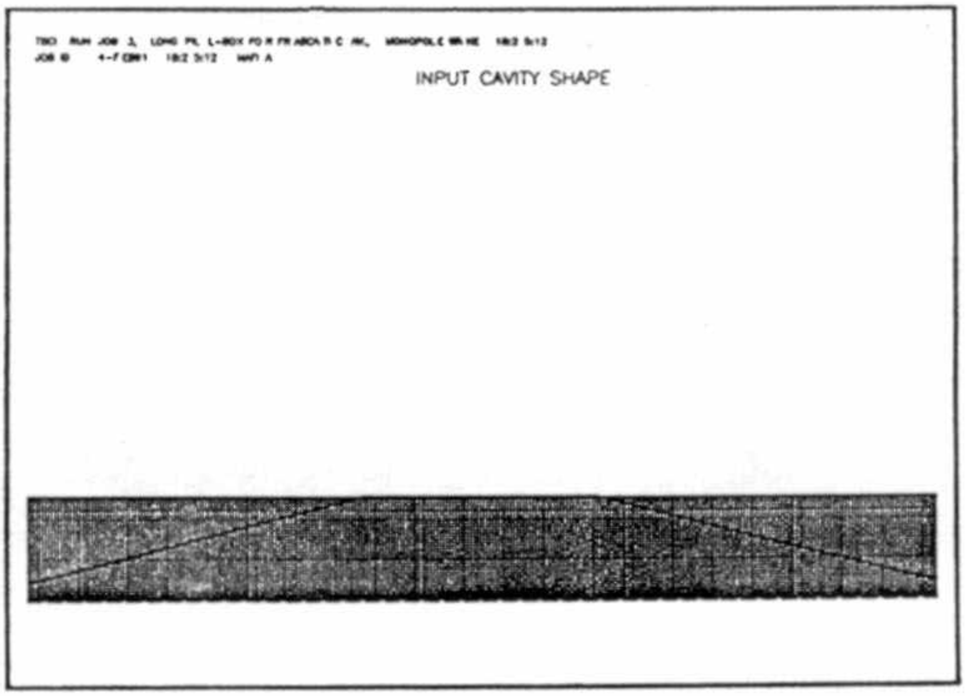

FIG 10

$K_T = 0.04$ V/pC

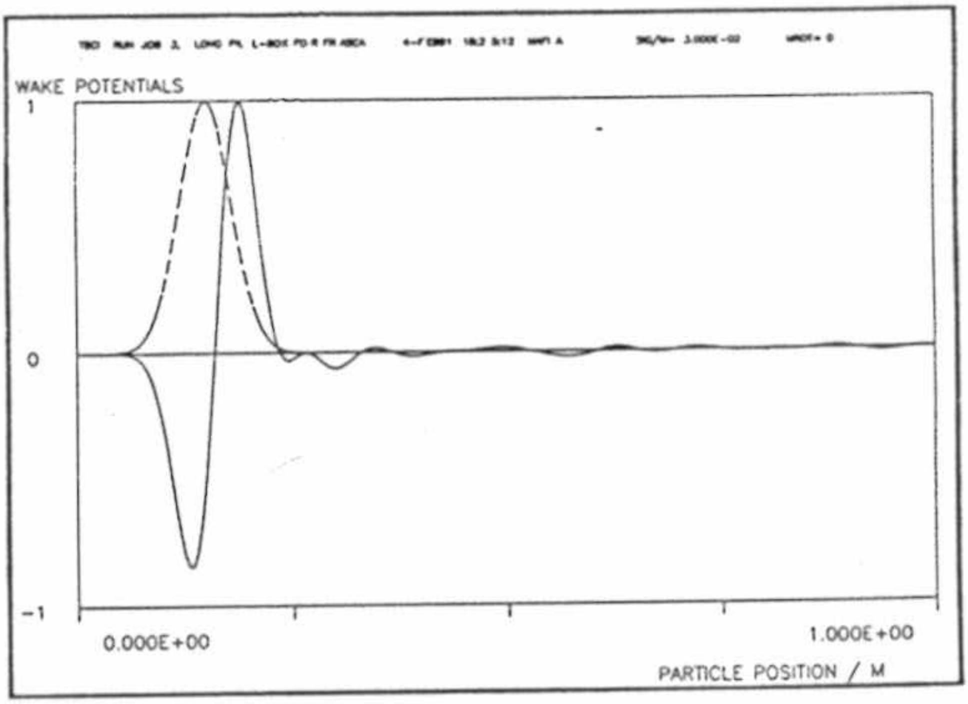

FIG 11

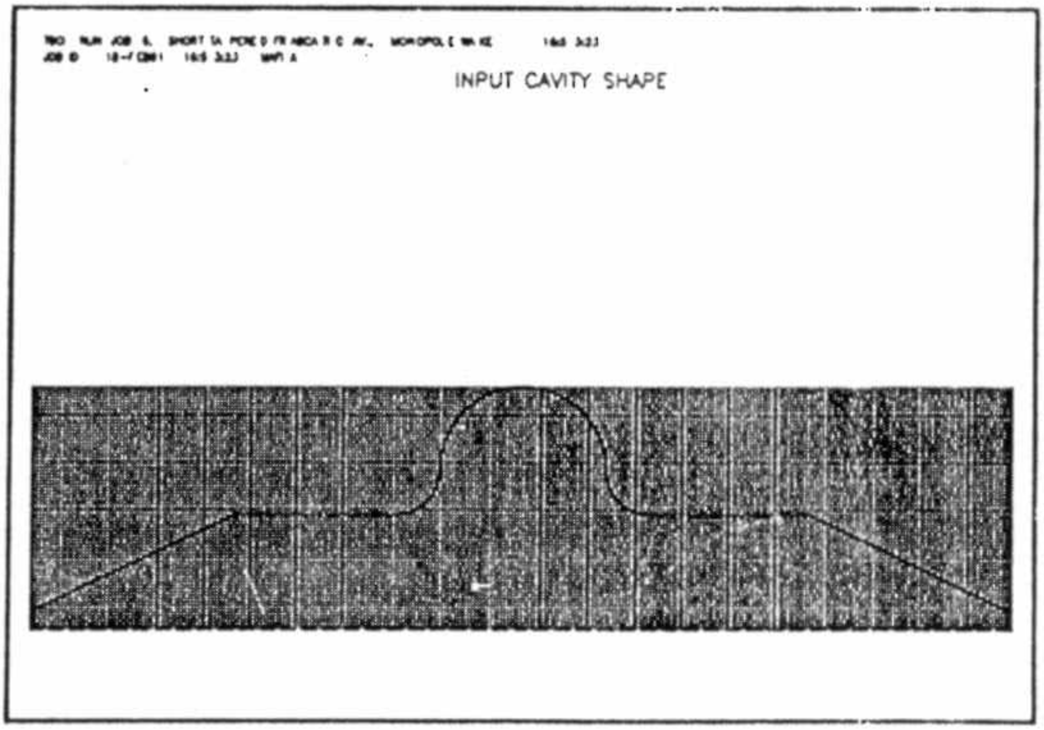

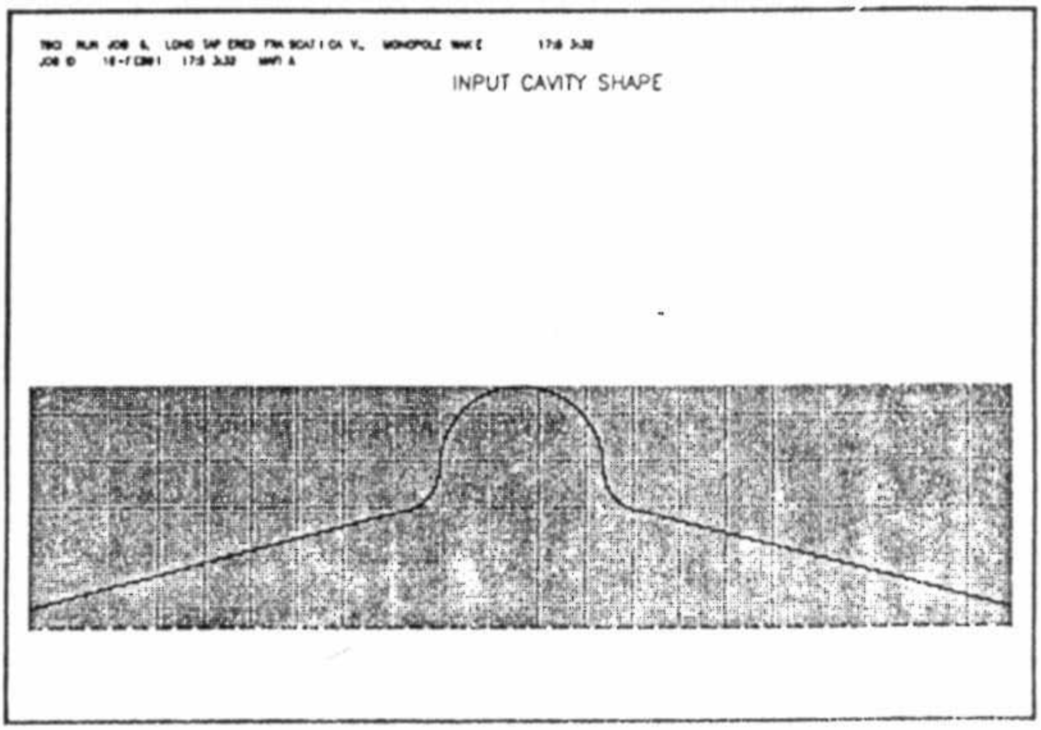

FIG 12

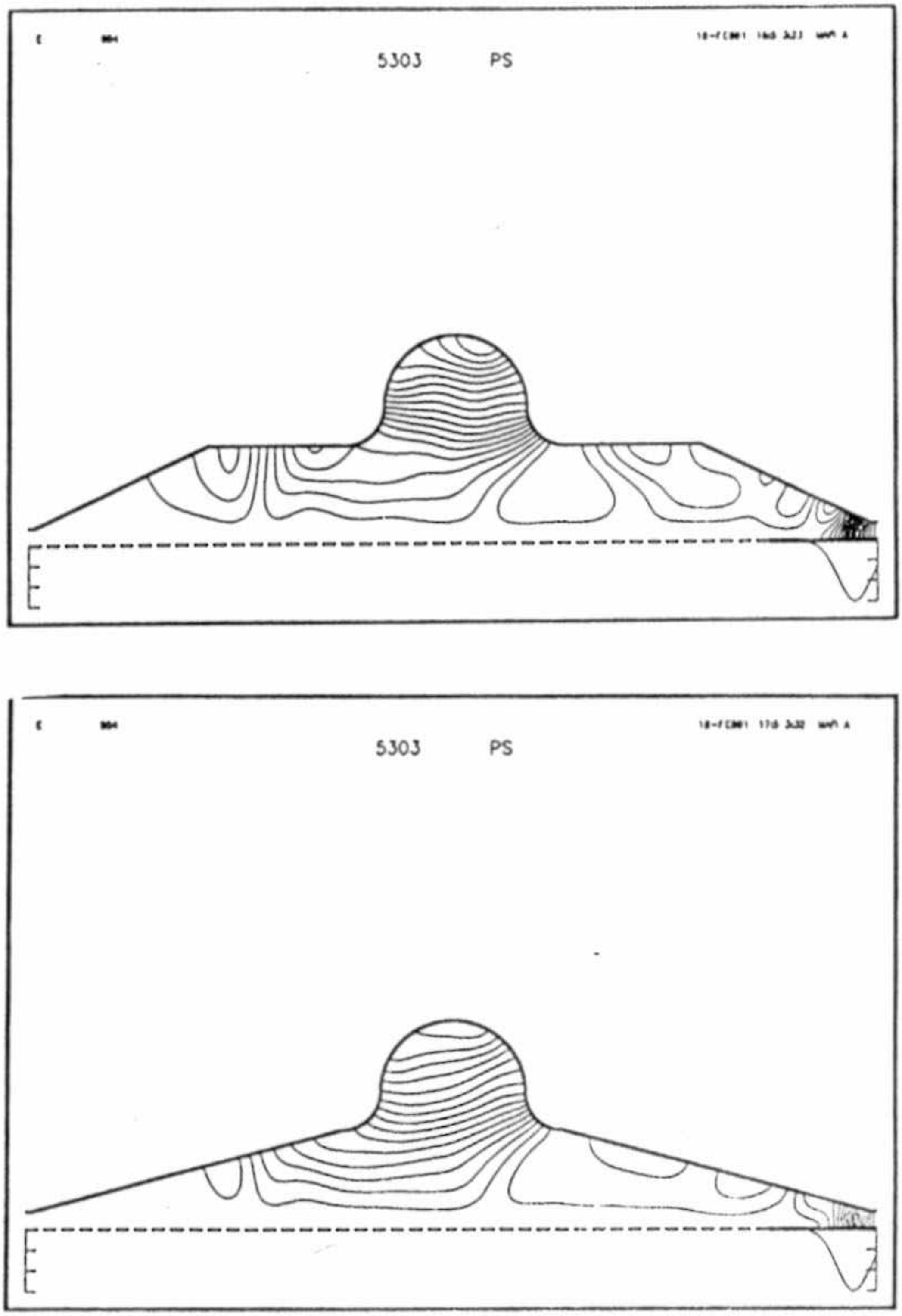

FIG 13

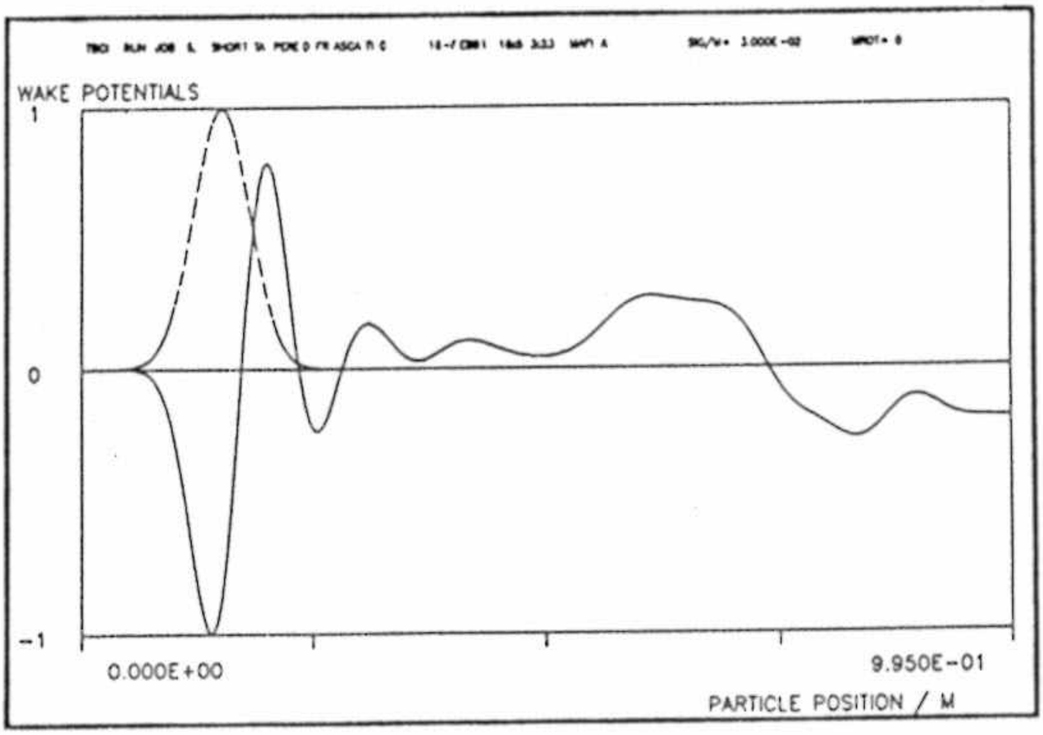

$k_T = 0.21$

$k_{pm} = 0.16$

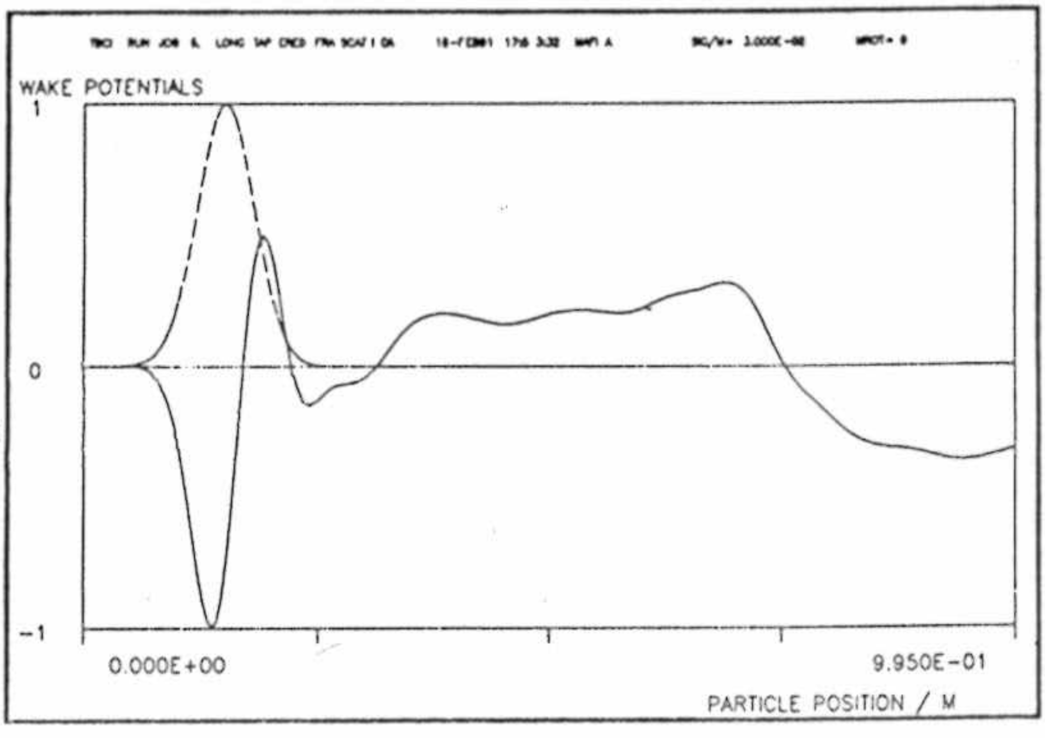

$k_T = 0.12$

$k_{pm} = 0.07$

FIG 14

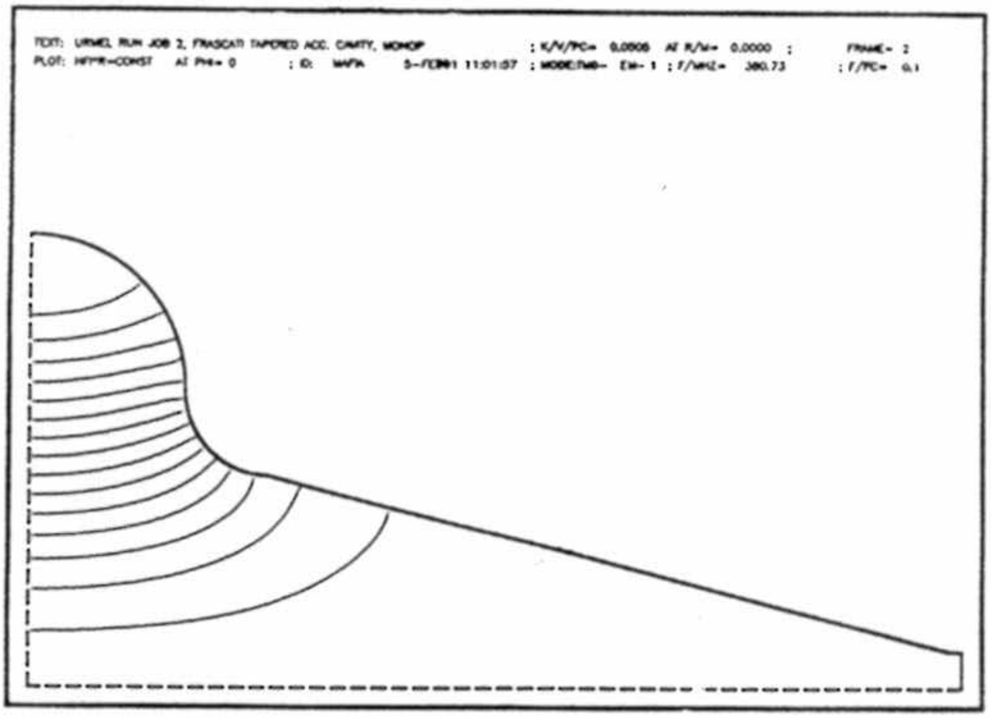
; K/V/PC= 0.0006 AT R/M= 0.0000 ;
FRAME= 2
PLOT: HFPR=CONST AT PHI= 0
F/MHZ= 380.73
; F/PC= 0.1

FIG 15

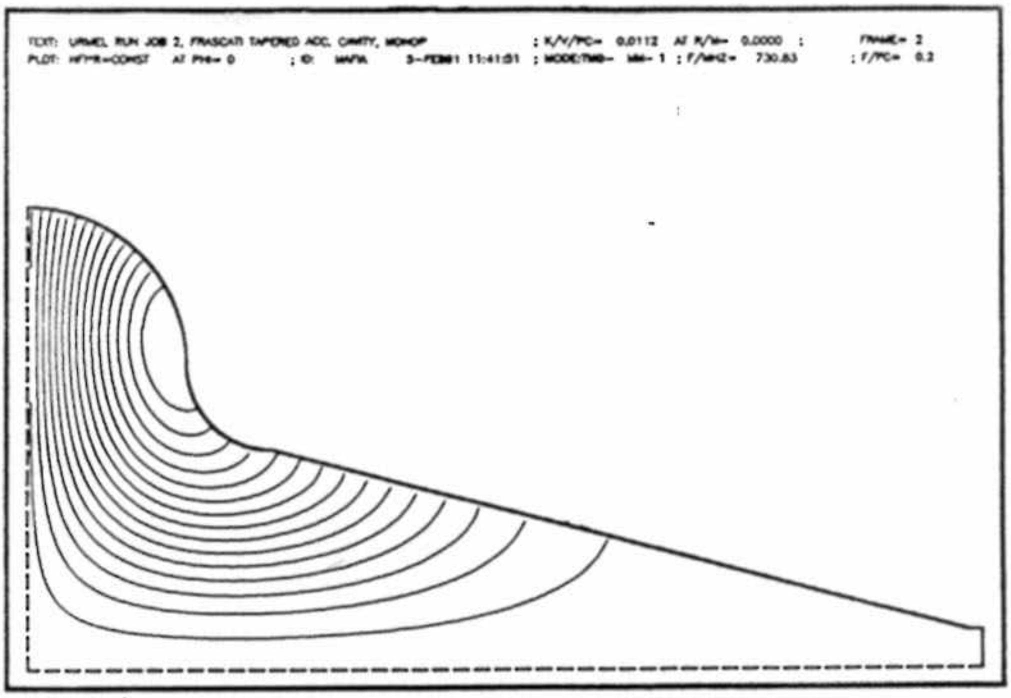
; K/V/PC= 0.0112 AT R/M= 0.0000 ;
FRAME= 2
PLOT: HFPR=CONST AT PHI= 0
F/MHZ= 730.83
; F/PC= 0.2

FIG 16